Engineering Properties of Mangking Sandstone

Ainuddin Yasin[1] and Jasmi Ab Talib[1]
[1]*Department of Geoscience Universiti Teknologi PETRONAS, Perak, Malaysia*
E-mail: ainuddin_18001571@utp.edu.my

ABSTRACT: This project was intended to characterize the engineering properties of Mangking Sandstone Formation in Maran, Pahang. The main lithology is fine-grained white to light grey sandstone. The engineering properties of Mangking Sandstone was assessed by applying geological technique which is discontinuity survey and geomechanical techniques including Schmidt Hammer test, Acoustic Velocity test, Uniaxial Compressive Strength (UCS) test, Brazilian Tensile Strength test and Point Load Strength test. The Rock Mass Rating (RMR) system was applied to the rock mass based on its geological discontinuity and geomechanical information to assess the quality of the rock. Slope Mass Rating (SMR) was applied to assess the stability of the slope. The RMR values range from 73 to 78 which place the Mangking Sandstone in Maran area in Class II (good rock). The SMR values place the rock slope of Mangking Sandstone in Maran area in Class II (stable slope).

KEYWORDS: Sandstone, Geology, Geomechanics, Mangking, Engineering.

1. INTRODUCTION

The evaluation of Mangking Sandstone in terms of engineering properties could give a huge contribution to the overall geological study of the Tembeling Group as it covers up a wide of approximately 60 percent in Maran area (Tate et al., 2008). Geological and geomechanical investigation are the pillars in conducting engineering geological assessment. One of the approaches done in geological investigation for this area is the use of discontinuity survey procedure to analyze important characteristics and features of the discontinuities.

The geomechanical investigation was carried out to test the physical strength of the rock mass. Acoustic Velocity test was carried out to evaluate the elastic properties of rock. Four geomechanical tests were applied which involves the Uniaxial Compressive Strength (UCS) test, Brazilian Tensile Strength test, Point Load Strength test and Schmidt Hammer test. This information, along with the information from the discontinuity survey were used in calculating the RMR.

RMR is a rating system developed to assess the quality of a rock mass based on six main parameters which include the strength of rock material, Rock Quality Designation (RQD), discontinuity spacing, discontinuity condition, groundwater condition, and orientation of discontinuities (Bieniawski, 1989).

The rock slopes were assessed by Slope Mass Rating (SMR) which analyze the rock slope stability and predict the type of failure that could occur along the discontinuity surface (Romana, 1985). The rating of the rock mass from these two systems could help project developers and engineers to have some insight on the safety and suitability of the site if any constructions and developments are planned to be done there.

The study area is located in Maran on the roadside of Jalan Kampung Belimbing. It is situated about 11 km from Maran town centre. Three localities were picked from a 300 m rock slope for assessment. The map of the study area and localities in Maran district are shown in Figure 1 and Figure 2, respectively.

2. METHODOLOGY

2.1 Discontinuity Survey

Discontinuity survey was carried out to characterize the discontinuities on the outcrops including discontinuity type, orientation, persistence, aperture, fill materials, roughness and water presence. These are the standard parameters in conducting discontinuity surveys (ISRM, 1981; Bartlett et al., 1998). A scanline made of measuring tape was laid on the outcrops surface and readings were obtained from the discontinuities that intercept the measuring tape (Bartlett et al., 1998; Mohamad et al., 2005).

2.2 Geomechanical Tests

Schmidt Hammer readings were acquired from the outcrop as one of the geomechanical techniques applied. By using the American Society for Testing Material (ASTM) standard, the Schmidt hammer was placed on smooth rock surfaces of dominant lithology and about 30 readings were acquired per locality. The mean reading for each locality was then recorded and plotted into the conversion chart proposed by Deere and Miller (1966). This chart was used to find the estimated UCS value of the rock.

The rock samples were cored into specific dimensions for different tests. Acoustic Velocity Test is a sonic log test on the rock cores intended to obtain the P-wave and S-wave velocity of the rock material. The test was conducted using OYO Sonic Viewer-SX adhering to Japan Quality Assurance Organization (JQA) standard. The frequency used for the test is about 200 kHz for P-wave and 100 kHz for S-wave. From the wave's velocities, elastic properties of the rock could be obtained including the Poisson's ratio (μ) of the rock and Young's Modulus (E) based on Mavko et al. (2003). These properties could help in determining the rock formation behavior.

Uniaxial Compressive Strength (UCS) test was done by placing a cylindrical core vertically under the load of the UCS machine. A computer was connected to the machine to calculate the load needed to break the core. The load was included with the area of the cylindrical core in Eq. (1) to calculate the UCS of the rock (ASTM, n.d.).

$$UCS = \frac{Load\ (MPa)}{Area} \quad (1)$$

Brazilian Tensile Strength test was conducted to measure the tensile strength of the rock. From the tensile strength, UCS value could be estimated by assuming that the compressive strength of a rock is approximately ten times greater than its tensile strength (Farmer, 1983; Sheorey, 1997). For this test, four disc-shaped cores for each locality were extracted from the rock sample. Increasing load was applied at a constant rate until the disc-shaped core was split. The splitting tensile strength, σ was calculated using Eq. (2) (ISRM, 1978; ASTM, 2008) where P is the maximum load applied when the core split, L is the core length in mm and D is the diameter of the core.

$$\sigma = \frac{2P}{\pi LD} \quad (2)$$

The Point Load Strength test was conducted on rock cores with lengths shorter than the ones used in the UCS test. The load in kN at which the cores started to undergo failure was recorded by the Point Load machine. The Point Load Index, *I* was then calculated using Eq. (3) (ASTM, n.d.).

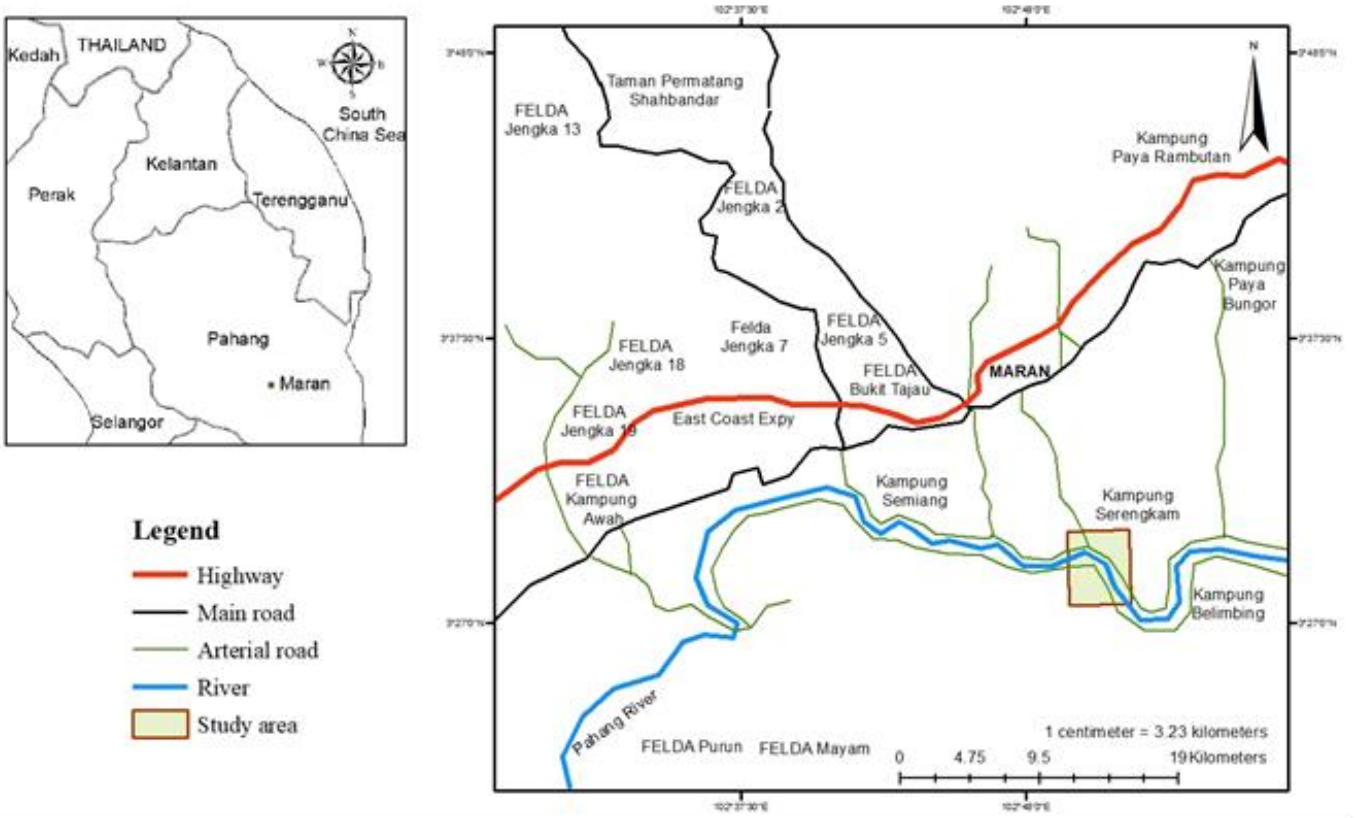

Figure 1 The map shows the study area located in Maran district

$$Point\ Load\ Index, I = \frac{Load\ in\ kN}{(diameter\ of\ core\ in\ mm)^2} \quad (3)$$

The correction factor, F was derived based on the diameter of the cores through Eq. (4) (ASTM, n.d.).

$$Correction\ Factor, F = \left(\frac{diameter\ in\ mm}{50}\right)^{0.45} \quad (4)$$

UCS value could be estimated from Point Load Strength test by finding the corrected Point Load Index, I_{S50} using Eq. (5) and Eq. (6) (ASTM, n.d.; Bieniawski, 1975) where,

$$Corrected\ Point\ Load\ Index, I_{S50} = I * F \quad (5)$$

$$Estimated\ UCS\ \ (Sedimentary\ Rocks) = 16 * I_{S50} \quad (6)$$

2.3 Rock Mass Rating (RMR)

Rock Mass Rating (RMR) is a rating system developed based on 6 main parameters including Uniaxial Compressive Strength (UCS) of rock material, Rock Quality Designation (RQD) of rock, spacing of discontinuities, condition of discontinuities, groundwater conditions and orientation of discontinuities (Bieniawski, 1989). For this project, UCS values were obtained from geomechanical tests including the UCS test, Brazilian Tensile Strength test, Point Load Strength test and Schmidt Hammer reading. The actual UCS value was combined with the estimated UCS values in Eq. (7) that weigh in actual UCS, where the actual UCS came from the UCS test and estimated UCS came from the rest of the geomechanical tests.

$$UCS\ value = \frac{\left(\frac{estimated\ UCS}{3}\right) + Actual\ UCS}{2} \quad (7)$$

RQD value was obtained from the discontinuity survey data. Adapting the RQD formulae in Eq. (8) and Eq. (9) (Farmer, 1983; ASTM, 2008), RQD was calculated by,

$$RQD = \frac{sum\ of\ the\ length\ of\ spacing\ more\ than\ 0.1\ m}{Total\ scanline\ length}\% \quad (8)$$

$$RQD = 100(0.1\lambda + 1)e^{(-0.1)\lambda} \quad (9)$$

λ is the total number of discontinuity readings over the scanline length. The lower RQD value was taken to be assigned in the RMR. Spacing of discontinuity was acquired by averaging the true spacings of each joint set on the outcrop. Condition of discontinuity includes persistence or discontinuity length, aperture, roughness, fill material and weathering condition. Groundwater condition was assessed by observing any presence of water along the discontinuities that could be sourced from the natural groundwater below the surface. Specific ratings were given for certain range of values for each parameter (Bieniawski, 1989).

2.4 Slope Mass Rating (SMR)

SMR was acquired from the calculation of RMR with specific adjustment factors (Romana, 1985). The orientation of discontinuity data was acquired by taking the readings of dip direction and dip amount of discontinuities in the discontinuity survey. The planar and toppling failures of each joint set together with the wedge failures (if any) on the outcrops were rated in the SMR system by evaluating the adjustment factors. The adjustment factors could be obtained from the measurement of the orientation of the main slope and discontinuities on the outcrop.

The adjustment factors were denoted as F1, F2, F3 and F4 in which F1 represents the rating given based on the dip direction of discontinuities and main slope (Value A), F2 represents the rating given based on dip amount of discontinuities (Value B) and F3 represents the rating given based on dip relationship between discontinuities and the slope (Value C). F4 represents the rating given based on how the outcrop is exposed, either through natural occurrence, blasting or presplitting (Romana, 1985). As the evaluation of the adjustment factors was completed, the SMR was calculated using Eq. (10) (Romana, 1985).

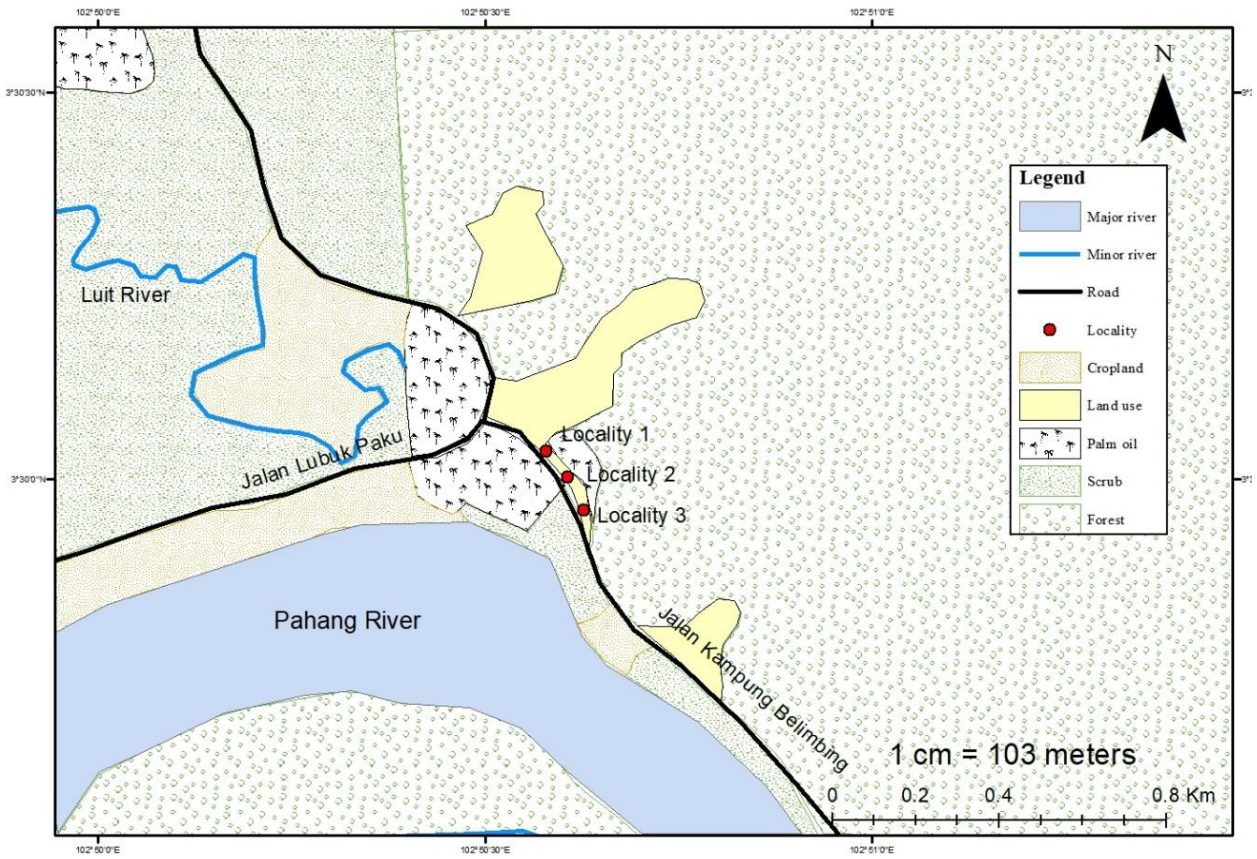

Figure 2 Locality map for the study area shows three localities that were evaluated in this study. These three localities combined to form a big rock slope that lies by the roadside of Jalan Kampung Belimbing within the coordinates of 3°30`03" N, 102°50'33" E

3. RESULTS AND DISCUSSION

3.1 Discontinuity Analysis

3.1.1 Locality 1

There are 6 discontinuity sets in locality 1. The average true spacing for locality 1 is 2.32 m. Set 1 to set 5 are mainly dominated by bedding planes as the major type of discontinuity. Joints of set 6 record the lowest value for average discontinuity length which is about 0.13 m. All six sets for this locality have discontinuities with moderate narrow to tight aperture. the unbounded fractures have a quite large range of aperture which is from moderate wide to tight. The discontinuities of the sets are mostly either discolored or filled with non-cohesive material mainly of sands. Most of the sets consist of discontinuities with rough surface except for set 1 with wavy surface and set 2 with smooth surface. There is no sign of water presence on the discontinuities for all sets. Generally, most of the discontinuities from Locality 1 come from bedding planes with moderate narrow aperture (20 mm – 60 mm), rough surfaces, discolored due to weathering and no presence of water. The summary of the analysis was shown clearly in Table 1 and Table 2.

3.1.2 Locality 2

There are 5 discontinuity sets in locality 2. The average true spacing for locality 2 is 3.68 m. Set 1 to set 4 are mainly dominated by bedding planes as the major type of discontinuity. Meanwhile, set 5 is dominated by fractures on the outcrop. The unbounded discontinuities are mainly caused by random and scattered fractures on the outcrop. In terms of the average length of discontinuity, bedding planes of set 4 record the highest reading among the other sets with the value of 3.9 m. Fractures of set 5 record the lowest value for average discontinuity length which is about 0.32 m. All five sets for this locality have discontinuities with moderate wide to very narrow aperture. The unbounded fractures have extremely narrow apertures generally. The discontinuities of the sets are mostly either discolored or filled with non-cohesive material mainly of sand grains. Only discontinuity in set 3 is considered clean as its aperture is extremely narrow and minimum to no sign of weathering spotted there. Most of the sets consist of discontinuities with wavy surfaces except for set 4 with rough surfaces and set 5 with smooth surfaces. There is no sign of water presence on the discontinuities for all sets. Generally, most of the discontinuities have a very narrow aperture (2 mm to 6 mm) with wavy surfaces, filled with non-cohesive materials that are sand grains and no presence of water. The summary of the analysis was shown clearly in Table 3 and Table 4.

3.1.3 Locality 3

There are 3 discontinuity sets in locality 3. The average true spacing for locality 3 is 4.12 m. Set 1 and set 2 are mainly dominated by bedding planes as the major type of discontinuity. Meanwhile, set 3 is dominated by fractures on the outcrop. In terms of the average length of discontinuity, bedding planes of set 2 record the highest reading among the other sets with the value of 4.29 m. Fractures of set 3 record the lowest value for average discontinuity length which is about 0.70 m. All three sets for this locality have discontinuities with narrow to tight aperture. The unbounded fractures have extremely narrow apertures generally. The discontinuities of the sets are mostly discolored except for set 1 discontinuity which is mainly filled with non-cohesive materials (sands). Most of the sets consist of discontinuities with wavy surface except for set 2 with smooth surface. There is no sign of water presence on the discontinuities for all sets. Generally, as a big portion of readings comes from Set 1, the discontinuities for the locality mostly have a narrow aperture (6 mm – 20 mm), filled with non-cohesive materials including sand grains and transported crushed mudstones, rough surfaces and dry condition. The summary of discontinuity analysis was shown clearly in Table 5 and Table 6 for locality 3.

Table 1 The apparent and true spacings of each discontinuity set along with the number of readings for each set of locality 1

Discontinuity Set No.	Dip Direction	Dip	No of Readings	Acute Angle	Apparent Spacing	True Spacing
1	127°	89°	17	77°	1.18 m	1.15 m
2	308°	67°	12	78°	1.67 m	1.50 m
3	160°	89°	10	70°	2.00 m	1.88 m
4	156°	83°	4	74°	5.00 m	4.77 m
5	156°	67°	7	74°	2.86 m	2.53 m
6	144°	57°	8	86°	2.50 m	2.09 m
Unbounded			42			

Table 2 The details of discontinuities for each set of Locality 1 including the type, average length, aperture, fill material, surface roughness and water condition

Discontinuity Set No.	Type of discontinuity	Average length	Aperture	Fill Material	Surface Roughness	Water Condition
1	Bedding Planes	0.64 m	Moderate narrow	Colored	Rough	Dry
2	Bedding Planes	0.35 m	Tight	Colored	Smooth	Dry
3	Bedding Planes	0.99 m	Moderate Narrow	Non-cohesive	Rough	Dry
4	Bedding Planes	0.18 m	Narrow	Colored	Rough	Dry
5	Bedding Planes	0.58 m	Moderate Narrow	Non-cohesive	Rough	Dry
6	Joint	0.13 m	Moderate Narrow	Non-cohesive	Rough	Dry
Unbounded	Fracture	0.39 m	Moderate Wide - Tight	Colored	Wavy	Dry

Table 3 The apparent and true spacings of each discontinuity set along with the number of readings for each set of Locality 2

Discontinuity Set No.	Dip Direction	Dip	No of Readings	Acute Angle	Apparent Spacing	True Spacing
1	158°	86°	11	82°	2.82 m	2.79 m
2	335°	89°	10	79°	3.10 m	3.04 m
3	281°	68°	8	25°	3.88 m	1.52 m
4	293°	76°	5	37°	6.20 m	3.62 m
5	180°	81°	4	76°	7.75 m	7.42 m
Unbounded			42			

Table 4 The details of discontinuities for each set of Locality 2 including the type, average length, aperture, fill material, surface roughness and water condition

Discontinuity Set No.	Type of discontinuity	Average length	Aperture	Fill Material	Surface Roughness	Water Condition
1	Bedding Planes	0.55 m	Very Narrow	Non-cohesive	Wavy	Dry
2	Bedding Planes	0.50 m	Very Narrow	Non-cohesive	Wavy	Dry
3	Bedding Planes	0.68 m	Extremely Narrow	Clean	Wavy	Dry
4	Bedding Planes	3.9 m	Moderate Wide	Non-cohesive	Rough	Dry
5	Fracture	0.32 m	Very Narrow	Colored	Smooth	Dry
Unbounded	Fracture	0.51 m	Extremely Narrow	Colored	Wavy	Dry

Table 5 The apparent and true spacings of each discontinuity set along with the number of readings for each set of Locality 3

Discontinuity Set No.	Dip Direction	Dip	No of Readings	Acute Angle	Apparent Spacing	True Spacing
1	285°	63°	25	23°	2.32 m	0.81 m
2	290°	83°	8	28°	7.25 m	3.38 m
3	169°	81°	7	87°	8.29 m	8.18 m
Unbounded			30			

Table 6 The details of discontinuities for each set of Locality 3 including the type, average length, aperture, fill material, surface roughness and water condition

Discontinuity Set No.	Type of discontinuity	Average length	Aperture	Fill Material	Surface Roughness	Water Condition
1	Bedding Planes	4.11 m	Narrow	Non-cohesive	Rough	Dry
2	Bedding Planes	4.29 m	Tight	Colored	Smooth	Dry
3	Fracture	0.70 m	Extremely Narrow	Colored	Rough	Dry
Unbounded	Cleavage	0.80 m	Extremely Narrow	Colored	Wavy	Dry

3.2 Geomechanical Analysis

3.2.1 Acoustic Velocity Test

Based on the results (Table 7), sandstone in Locality 2 exhibits the highest Young's Modulus value at 24.44 GPa followed by sandstone in Locality 1 at 17.01 GPa. The sandstone in Locality 3 was noted to have the lowest Young's Modulus value at just 5.34 GPa. These values of Young's Modulus suggested that the sandstone in Locality 2 is the stiffest in nature among the sandstones of the other 2 localities as the stiffness of a material is directly proportional to the Young's Modulus of a material (Yale and Swami, 2017; Onalo et al., 2018). Thus, the sandstone in Locality 2 requires the highest amount of stress for the rock to achieve a given amount of strain. Meanwhile, the sandstone in Locality 3 is the least stiff among the sandstones of the other localities based on Young's Modulus value.

Figure 3 The three rock cores from locality 1 used for the Acoustic Velocity test and UCS test

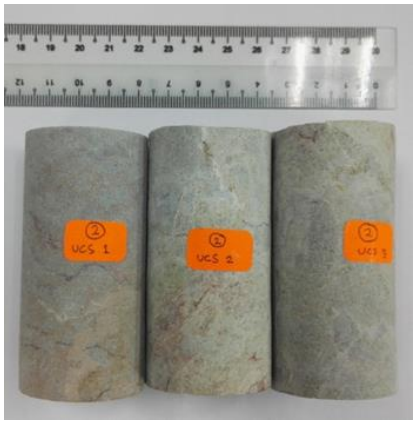

Figure 4 The three rock cores from locality 2 used for the Acoustic Velocity test and UCS test

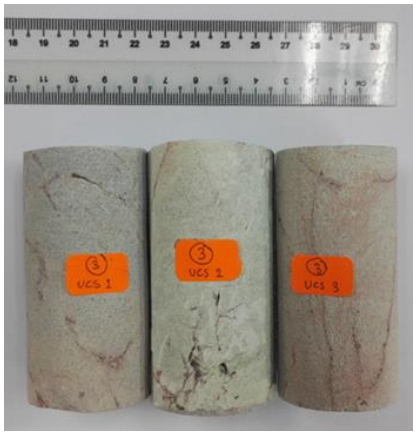

Figure 5 The three rock cores from locality 3 used for Acoustic Velocity test and UCS test

Table 7 The elastic properties of rock materials based on the acoustic velocities

Locality 1		
Core Number	**Poisson's Ratio, μ**	**Young's Modulus, E**
1	0.408	6.19 GPa
2	0.267	23.98 GPa
3	0.130	20.85 GPa
Average Value	0.268	17.01 GPa
Locality 2		
Core Number	**Poisson's Ratio, μ**	**Young's Modulus, E**
1	0.274	25.01 GPa
2	0.271	23.18 GPa
3	0.303	25.13 GPa
Average Value	0.283	24.44 GPa
Locality 3		
Core Number	**Poisson's Ratio, μ**	**Young's Modulus, E**
1	0.429	4.00 GPa
2	0.338	9.58 GPa
3	0.439	2.43 GPa
Average Value	0.402	5.34 GPa

The sandstones in Locality 1 and Locality 2 were classified as medium sandstone based on the typical range of Young's Modulus value for different types of rocks which is between 13.8 to 34.5 GPa (Lake, 2007). Sandstone in Locality 3 was considered as soft sandstone in which the range of soft sandstone is between 0.7 to 6.9 GPa (Lake, 2007). For Poisson's ratio value, the sandstone in Locality 3 displays the highest value at 0.402. This value is quite high even for a soft sandstone as Poisson's ratio for typical soft sandstone only ranges from 0.2 to 0.35. The sandstone in Locality 1 noted the lowest value of Poisson's ratio at only 0.268 closely followed by the sandstone of Locality 2 at 0.283.

Sandstone in Locality 3 was expected to have the lowest unconfined compressive strength and tensile strength value due to the high Poisson's ratio (D'Andrea et al., 1965).

3.2.2 Uniaxial Compressive Strength (UCS) Test

The core diameters for all specimens are 37 mm (Figures 6-8). Based on the results (Tables 8-10), the sandstone in Locality 2 is the strongest among the three localities with an average UCS value of 131.51 MPa followed by sandstone in Locality 1 with an average UCS value of 71.39 MPa. Locality 3 sandstone recorded the lowest average UCS value at only 28.55 MPa. This result somewhat corresponded to the elastic properties evaluation from the Acoustic Velocity test where the sandstone in Locality 2 marked the highest Young's Modulus value followed by Locality 1 and Locality 3 as having the lowest Young's Modulus value. This information further strengthens the theory that UCS value is increasing with increasing Young's Modulus (Carmichael, 1982; Jizba, 1991).

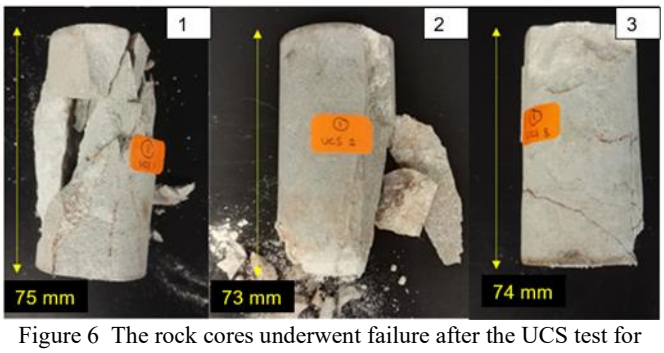

Figure 6 The rock cores underwent failure after the UCS test for Locality 1

Table 8 The UCS values for the rock cores in Locality 1

Core Number	UCS Value
1	79.27 MPa
2	55.02 MPa
3	79.87 MPa
Average	**71.39 MPa**

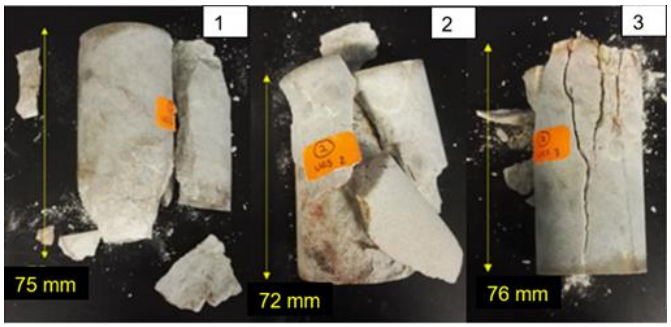

Figure 7 The rock cores underwent failure after the UCS test for Locality 2

Table 9 The UCS values for the rock cores in Locality 2

Core Number	UCS Value
1	155.15 MPa
2	135.56 MPa
3	103.82 MPa
Average	**131.51 MPa**

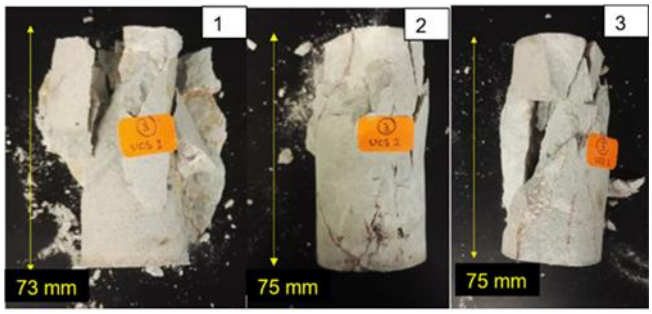

Figure 8 The rock cores underwent failure after the UCS test in Locality 3

Table 10 The UCS values for the rock cores for Locality 3

Core Number	UCS Value
1	31.57 MPa
2	24.78 MPa
3	29.31 MPa
Average	**28.55 MPa**

3.2.3 Brazilian Tensile Strength Test

The core diameters for all specimens are 49 mm (Figures 9-11). Based on the Brazilian Strength test results (Tables 11-13), the cores in Locality 2 achieved the highest average tensile strength value with 7.347 MPa followed by the cores in Locality 1 with a tensile strength value of 4.304 MPa. The cores in Locality 3 recorded the lowest tensile strength value at only 2.729 MPa. Once the Unconfined Compressive Strength (UCS) values were estimated from the average tensile strength values (Farmer, 1983; Sheorey, 1997), the cores in Locality 1, Locality 2 and Locality 3 recorded estimated UCS values at 43.04 MPa, 73.47 MPa and 27.29 MPa, respectively. The difference in values between actual UCS and estimated UCS could be caused by the heterogenous nature of the sandstone in terms of fracturing and mineral arrangements in which highly fractured rocks and loosely arranged minerals will give a lower strength value even though they were extracted from the same area. However, the differences between estimated and actual UCS values is not too high to the point where the Brazilian tensile strength test become unreliable. The differences in values for those three localities are still below 100 MPa hence, the Brazilian tensile strength test is still reliable to be used to estimate UCS values.

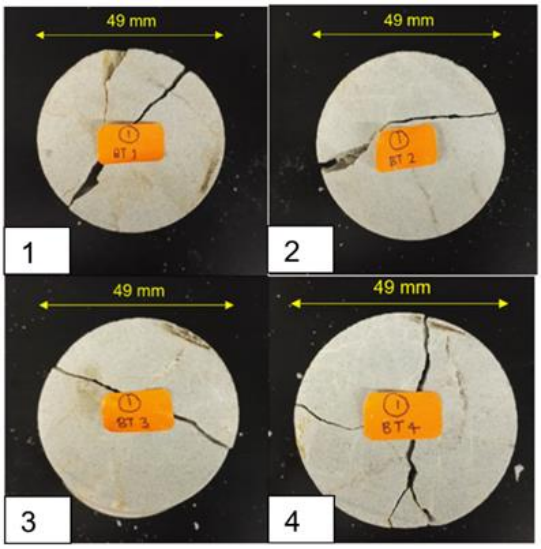

Figure 9 The disc-shaped rock cores underwent failure after the Brazilian Tensile Strength test for Locality 1

Table 11 The tensile strength value along with the estimated UCS for rock cores in Locality 1

Core Number	Tensile strength
1	5.425 MPa
2	3.771 MPa
3	3.530 MPa
4	4.491 MPa
Average	**4.304 MPa**
	Estimated UCS = 43.04 MPa

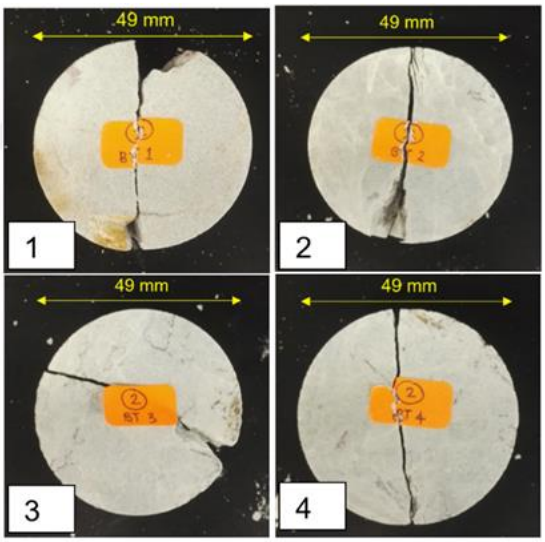

Figure 10 The disc-shaped rock cores underwent failure after the Brazilian Tensile Strength test for Locality 2

Table 12 The tensile strength value along with the estimated UCS for rock cores in Locality 2

Core Number	Tensile strength
1	3.998 MPa
2	8.177 MPa
3	7.684 MPa
4	9.527 MPa
Average	**7.347 MPa**
	Estimated UCS = 73.47 MPa

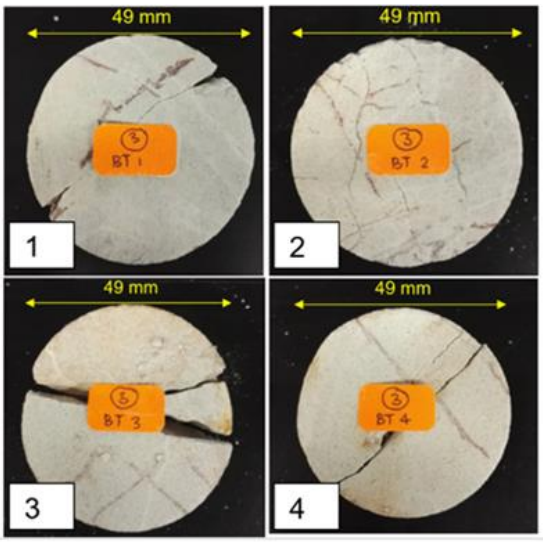

Figure 11 The disc-shaped rock cores underwent failure after the Brazilian Tensile Strength test for Locality 3

Table 13 The tensile strength value along with the estimated UCS for rock cores in Locality 3

Core Number	Tensile strength
1	5.244 MPa
2	3.279 MPa
3	1.356 MPa
4	1.038 MPa
Average	**2.729 MPa**
	Estimated UCS = 27.29 MPa

3.2.4 Point Load Strength Test

The core diameters for all specimens are 37 mm (Figures 12-14). Based on the Point Load Strength test results (Tables 14-16), the cores in Locality 2 achieved the highest average estimated UCS value with 155.24 MPa followed by the cores in Locality 1 with an average estimated UCS value of 45.152 MPa. The cores in Locality 3 recorded the lowest average estimated UCS value at only 20.40 MPa.

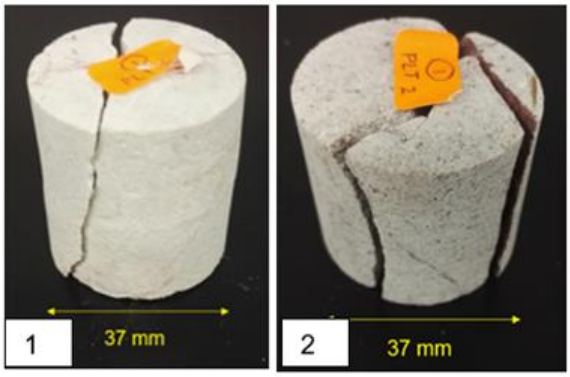

Figure 12 The rock cores from locality 1 prepared for the Point Load Strength test

Table 14 The point load index values along with the correction factor, corrected index and estimated UCS for rock cores in Locality 1

	Core 1	Core 2
Point Load Index, I	3.961 MPa	2.460 MPa
Correction Factor, F	0.879	0.879
Corrected Point Load Index, I_{S50}	3.482 MPa	2.162 MPa
Estimated UCs	55.712 MPa	34.592 MPa
Average UCS	**45.152 MPa**	

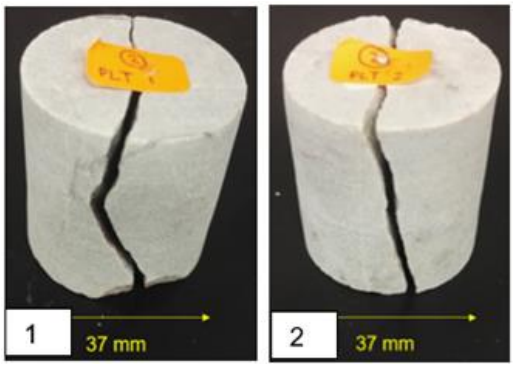

Figure 13 The rock cores from locality 2 prepared for the Point Load Strength test

Table 15 The point load index values along with the correction factor, corrected index and estimated UCS for rock cores in Locality 2

	Core 1	Core 2
Point Load Index, I	11.85 MPa	10.226 MPa
Correction Factor, F	0.879	0.879
Corrected Point Load Index, I_{S50}	10.416 MPa	8.989 MPa
Estimated UCs	166.66 MPa	143.82 MPa
Average UCS	**155.24 MPa**	

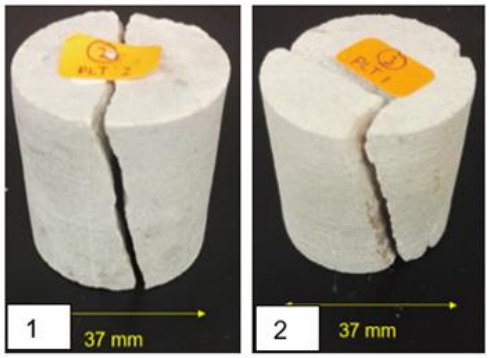

Figure 14 The rock cores from locality 3 prepared for the Point Load Strength test

Table 16 The point load index values along with the correction factor, corrected index and estimated UCS for rock cores in Locality 3

	Core 1	Core 2
Point Load Index, I	1.429 MPa	1.472 MPa
Correction Factor, F	0.879	0.879
Corrected Point Load Index, I_{S50}	1.256 MPa	1.294 MPa
Estimated UCs	20.10 MPa	20.70 MPa
Average UCS	**20.40 MPa**	

The huge difference in values between actual UCS and estimated UCS from both Brazilian Tensile Strength test and Point Load strength test like mentioned before, could be caused by the heterogenous nature of the sandstone in terms of fracturing and mineral arrangements in which highly fractured rocks and loosely arranged minerals will give a lower strength value even though they were extracted from the same area.

3.2.5 Schmidt Hammer Test

The UCS range of sandstone is 20 -170 MPa (Jackson School of Geoscience, n.d.) Based on the results obtained from three localities (Table 17), the rocks of Mangking Sandstone are varied in strength. Among the three localities, the rock in the second locality exhibits the highest estimated UCS value (121 MPa) and was considered as hard sandstone while the rock in the third locality exhibits the lowest

estimated UCS value (33 MPa) and is considered as soft sandstone. The rock in the first locality was considered ~~as~~ intermediate in terms of strength with a value of 74 MPa. This difference in strength values could be the result of different mineral compositions of the sandstones, grain size and fractures present.

From Eq. (7), the UCS weighed in for locality 1 is 56.23 MPa, 109.87 MPa for locality 2 and 27.2 MPa for locality 3.

Table 17 The average Schmidt Hammer value along with estimated UCS for rock cores in Locality 1,2 and 3

Locality	Unit Weight of Rock (kN/m^3)	Average Schmidt Hammer Value	Estimated UCS Value (MPa)
1	25.4	39	74
2	26.3	47	121
3	24.5	21	32

3.3 Rock Mass Rating (RMR)

The values of RMR for the three localities range from 73 to 78 (Tables 18-20) which place the Mangking Sandstone rock in Class II (Bieniawski, 1979). Class II rock is considered a good rock with an average stand-up time of about 1 year for 10 m span. This means if the rock mass is tunneled for a 10 m span without any supports installed, it could withstand approximately 1 year from the period of tunneling. The rock mass cohesion is high which is in the range of 300 – 400 kPa. This value is good and somewhat proves the stability of the slope. The rock mass friction angle is in the range of 35° to 45° which is high. This indicates that the rock unit of Mangking Sandstone in Maran area could withstand a large magnitude of shear stress.

Table 18 The RMR calculation from the 5 parameters in Locality 1

Item	Value	Rating
UCS	56.23 MPa	7
RQD	90.98%	20
Spacing of Discontinuity	2.32 m	20
Condition of Discontinuity	Persistence (0.46 m)	6
	Aperture (20 – 60 mm)	0
	Roughness (Rough)	5
	Infilling (Hard < 5 mm)	4
	Weathering (Highly)	1
Groundwater Condition	Dry	15
RMR		78

Table 19 The RMR calculation from the 5 parameters in Locality 2

Item	Value	Rating
UCS	109.87 MPa	12
RQD	98.31%	20
Spacing of Discontinuity	3.68 m	20
Condition of Discontinuity	Persistence (1.08 m)	4
	Aperture (2 – 6 mm)	1
	Roughness (Slightly Rough)	3
	Infilling (Hard > 5 mm)	2
	Weathering (Highly)	1
Groundwater Condition	Dry	15
RMR		78

Table 20 The RMR calculation from the 5 parameters in Locality 3

Item	Value	Rating
UCS	27.2 MPa	7
RQD	99.3%	20
Spacing of Discontinuity	4.12 m	20
Condition of Discontinuity	Persistence (2.48 m)	4
	Aperture (6-20 mm)	0
	Roughness (Rough)	5
	Infilling (Hard > 5 mm)	2
	Weathering (Moderately)	3
Groundwater Condition	Dry	15
RMR		73

3.4 Slope Mass Rating (SMR)

Based on the Slope Mass Rating (SMR) evaluation (Tables 21-29), 2 joint interactions were found in locality 1. These two joint intersections fall in the critical zone which indicates them as possible wedge failures along the slope. These wedges were identified as W1 (087/42) and W2 (069/36). W2 is the one that contributes the largest adjustment factor value (F1.F2.F3) at - 35.7 which drops down the SMR value at a massive rate. The toppling failures of all 6 sets in locality 1 were valued at – 3.75 in terms of the adjustment factor. This shows that toppling failure has a very low chance to occur in locality 1. The largest adjustment factor value for planar failure in locality 1 is -9 at joint set 6 which means joint set 6 has the highest chance of developing planar failure along the discontinuity surface of locality 1.

In locality 2, the planar failure for all sets were valued at 0 in terms of the adjustment factor except for joint set 3. However, the value is relatively small hence indicating the rock slope of locality 2 to have a low chance of developing planar failure. For toppling failure in locality 2, joint set 3 recorded the largest adjustment factor value at -10. This made joint set 3 has the highest chance of developing toppling failure along the discontinuity surface of locality 2. In locality 3, 2 of the 3 joint sets recorded high values of adjustment factor for toppling failures at -10. These two joint sets are joint set 1 and joint set 2. Joint set 1 also has a relatively high chance to develop planar failure as the adjustment factor value reaches -7.5 which is the highest among the 3 sets.

Table 21 The A, B and values for each joint set. Given that dip direction and dip amount of slope is (50/68) and RMR = 78

Joint Plane/ Wedge	Type of Failure	A	B	C
1 (127/89)	Planar	77°	89°	21°
	Toppling	103°	89°	157°
2 (308/67)	Planar	258°	67°	- 1°
	Toppling	78°	67°	135°
3 (160/89)	Planar	110°	89°	21°
	Toppling	70°	89°	157°
4 (156/83)	Planar	106°	83°	15°
	Toppling	74°	83°	151°
5 (156/67)	Planar	106°	67°	- 1°
	Toppling	74°	67°	165°
6 (144/57)	Planar	94°	57°	- 11°
	Toppling	86°	57°	125°
W1 (087/42)	Wedge	37°	42°	- 26°
W2 (069/36)	Wedge	19°	36°	- 32°

Table 22 The F1, F2 and F3 values in locality 1

Joint Plane/ Wedge	Type of Failure	F1	F2	F3
1	Planar	0.15	1	0
	Toppling	0.15	1	- 25
2	Planar	0.15	1	- 50
	Toppling	0.15	1	- 25
3	Planar	0.15	1	0
	Toppling	0.15	1	- 25
4	Planar	0.15	1	0
	Toppling	0.15	1	- 25
5	Planar	0.15	1	- 50
	Toppling	0.15	1	- 25
6	Planar	0.15	1	- 60
	Toppling	0.15	1	- 25
W1	Wedge	0.15	0.85	- 60
W2	Wedge	0.7	0.85	- 60

Table 23 The F1, F2 and F3 multiplied in locality 1 to give the SMR values and the classes. Given that F4 = 0

Joint Plane/ Wedge	Type of Failure	F1*F2*F3	SMR	Class
1	Planar	0	78	II
	Toppling	- 3.75	74.25	II
2	Planar	- 7.5	70.5	II
	Toppling	- 3.75	74.25	II
3	Planar	0	78	II
	Toppling	- 3.75	74.25	II
4	Planar	0	78	II
	Toppling	- 3.75	74.25	II
5	Planar	- 7.5	70.5	II
	Toppling	- 3.75	74.25	II
6	Planar	-9	69	II
	Toppling	-3.75	74.25	II
W1	Wedge	- 7.65	70.35	II
W2	Wedge	- 35.7	42.3	III

Table 24 The A, B and C values for each joint set. Given that dip direction and dip amount of slope is (76/65) and RMR = 78

Joint Plane/ Wedge	Type of Failure	A	B	C
1 (158/86)	Planar	82°	86°	21°
	Toppling	98°	86°	151°
2 (335/89)	Planar	259°	89°	24°
	Toppling	79°	89°	154°
3 (281/68)	Planar	205°	68°	3°
	Toppling	25°	68°	133°
4 (293/76)	Planar	217°	76°	11°
	Toppling	37°	76°	141°
5 (180/81)	Planar	104°	81°	16°
	Toppling	76°	81°	146°

Table 25 The F1, F2 and F3 values in locality 2

Joint Plane/ Wedge	Type of Failure	F1	F2	F3
1	Planar	0.15	1	0
	Toppling	0.15	1	- 25
2	Planar	0.15	1	0
	Toppling	0.15	1	- 25
3	Planar	0.15	1	- 6
	Toppling	0.40	1	- 25
4	Planar	0.15	1	0
	Toppling	0.15	1	- 25
5	Planar	0.15	1	0
	Toppling	0.15	1	- 25

Table 26 The F1, F2 and F3 multiplied in locality 2 to give the SMR values and the classes. Given that F4 = 0

Joint Plane/ Wedge	Type of Failure	F1*F2*F3	SMR	Class
1	Planar	0	78	II
	Toppling	- 3.75	74.25	II
2	Planar	0	78	II
	Toppling	- 3.75	74.25	II
3	Planar	- 0.9	77.1	II
	Toppling	- 10	68	II
4	Planar	0	78	II
	Toppling	- 3.75	74.25	II
5	Planar	0	78	II
	Toppling	- 3.75	74.25	II

Table 27 The A, B and C values for each joint set. Given that dip direction and dip amount of slope is (82/67) and RMR = 73

Joint Plane/ Wedge	Type of Failure	A	B	C
1 (285/63)	Planar	203°	63°	- 4°
	Toppling	23°	63°	130°
2 (290/83)	Planar	208°	83°	16°
	Toppling	28°	83°	150°
3 (169/81)	Planar	87°	81°	14°
	Toppling	93°	81°	148°

Table 28 The F1, F2 and F3 values in locality 3

Joint Plane/ Wedge	Type of Failure	F1	F2	F3
1	Planar	0.15	1	- 50
	Toppling	0.4	1	- 25
2	Planar	0.15	1	0
	Toppling	0.4	1	- 25
3	Planar	0.15	1	0
	Toppling	0.15	1	- 25

Table 29 The F1, F2 and F3 multiplied in locality 3 to give the SMR values and the classes. Given that F4 = 0

Joint Plane/ Wedge	Type of Failure	F1*F2*F3	SMR	Class
1	Planar	- 7.5	65.5	II
	Toppling	- 10	63	II
2	Planar	0	73	II
	Toppling	- 10	63	II
3	Planar	0	73	II
	Toppling	- 3.75	69.25	II

Generally, from the SMR evaluation of the 3 localities representing Mangking Sandstone in Maran area, most of the joint sets fall in Class II (Romana, 1985). The exception was given to the wedge failure, W2 in locality 1 as the SMR value fell in Class III. Class II is given as the SMR value for all joint sets (except W2) were in the range between 61 to 80. The lowest SMR was recorded in toppling failures of joint set 1 and joint set 2 in locality 3 at 63 while the highest SMR value was recorded in planar failures of joint set 1, 3 and 4 in locality 1 and joint set 1,2,4 and 5 in locality 2 at 78. Wedge failure 2 (W2) in locality 1 recorded an SMR value of 42.3. Class II indicates that the rock slope of Mangking Sandstone in Maran area is stable with the probability of failure at only 0.2 (Romana, 1985).

4. CONCLUSIONS

Generally, most discontinuities from Locality 1 come from bedding planes with moderate narrow aperture (20 mm – 60 mm), rough surfaces, discolored due to weathering and no presence of water. In locality 2, most of the discontinuities have very narrow aperture (2 mm to 6 mm) with wavy surface, filled with sand grains and no presence of water. For locality 3, the discontinuities for the locality mostly have a narrow aperture (6 mm – 20 mm), filled with sand

grains and transported crushed mudstones, rough surfaces and dry conditions.

Based on the Acoustic Velocity test, rocks in locality 2 tend to be the stiffest among the three localities due to their highest value of Young's Modulus (Yale and Swami, 2017; Onalo et al., 2018). Rocks in locality 3 are the least stiff among the sandstones of the other localities.

The average UCS for Mangking Sandstone in Maran area is 77.15 MPa. The average tensile strength for Mangking Sandstone is 4.79 MPa, giving an estimated UCS value of 47.9 MPa. The average estimated UCS value from the Point Load Strength test for Mangking Sandstone is 73.6 MPa.

The average estimated UCS value obtained from the Schmidt Hammer test is 75.67 MPa. The estimated UCS values from multiple geomechanical techniques are almost similar to the actual UCS value except for the Brazilian Tensile Strength test. This could be due to the generalization of sandstone in the formula used to convert the tensile strength.

The values of RMR for the three localities range from 73 to 78 which place the Mangking Sandstone rock in Class II. Class II rock is considered a good rock with an average stand-up time of about 1 year for a 10 m spans, rock mass cohesion at 300 – 400 kPa and the rock mass friction angle is in the range of 35° to 45° which is high. This indicates that the rock unit of Mangking Sandstone in Maran area could withstand a large magnitude of shear stress (Bieniawski, 1979).

Generally, from the SMR evaluation of the 3 localities representing Mangking Sandstone in Maran area, most of the joint sets fall in Class II according to SMR developed by Romana (1985). Class II indicates that the rock slope of Mangking Sandstone in Maran area is stable with the probability of failure at only 0.2 (Romana, 1985).

With the rising modernization along with country population, the area of Central Pahang can be further developed for residential, commercial, and industrial purposes. Even though it would not become as bustling as the metropolitan areas along the West Coast, the need for engineering geology assessment is still not being secluded to minimize the risks of geological hazards. Engineering geology assessment could raise awareness regarding the impact of geology on infrastructural planning and development as well as a reminder to the community on how engineering geology is crucial in reducing the risks as result of human-environment interaction. From the results of SMR, the areas of Central Pahang those hose Mangking Sandstone as their foundation could have a good prospect for infrastructural development without much concern on structural integrity problems.

5. REFERENCES

American Society for Testing and Materials (ASTM) (2008) "Standard test method for splitting tensile strength of intact rock core specimens", ASTM International D 3967-08, West Conshohocken, USA.

American Society for Testing and Materials (ASTM) "Test Method for Unconfined Compressive Strength of Intact Rock Core Specimens", D 2938.

American Society for Testing and Materials (ASTM) "Standard method of test for elastic moduli of rock core specimens in uniaxial compression", ASTM Designation D 3148-72.

American Society for Testing and Materials (ASTM) (2014) "Standard Test Method for Determination of Rock Hardness by Rebound Hammer Method", ASTM International, West Conshohocken, PA D 5873-14.

Bartlett, S., Calcagno, F., Hill, M., Kunzer, S., Farrar, J., Hebenstreit, S., and Rohrer, P. (1998) "Engineering Geology Field Manual (Second Edition ed. Vol. 1)", U.S. Department of the Interior Bureau of Reclamation.

Bieniawski, Z.T. (1975) "The Point Load Test in Geotechnical Practice", Eng. Geol., September 1975, pp1-11.

Bieniawski, Z.T. (1979) "The Geomechanics Classification in Rock Engineering Application", Proceedings 4th International Congress on Rock Mechanics, Montreux, 2-8 September 1979, Vol. 2, pp41-48.

Bieniawski, Z.T. (1989) "Engineering rock mass classifications: a complete manual for engineers and geologists in mining, civil, and petroleum engineering", New York.

Carmichael, R. S. (1982) "Handbook of Physical Properties of Rocks", Vol. 2, Boca Raton: CRC Press.

D'Andrea, D., Fischer, R. L., and Fogelson, D. E. (1965) "Prediction of Compressive Strength from Other rock Properties", USBM, RI 6702.

Deere, D. U. (1964) "Technical description of rock cores", Rock Mechanics Engineering Geology, 1, pp16-22.

Farmer, I.W. (1983) "Engineering Behavior of Rocks", London, Chapman and Hall.

Hudson, J. A., and Harrison, J. P. (1997) "Engineering Rock Mechanics - An Introduction to the Principles", Elsevier Science, Oxford.

International Society for Rock Mechanics (ISRM) (1978) "Suggested Methods for Determining Tensile Strength of Rock Materials", Int J Rock Mech Min Sci Geomech Abstr, 15(3), pp99–103. doi:10.1016/0148-9062(78)90003-7

International Society for Rock Mechanics (ISRM) (1981) "Rock Characterization Suggested Method", Testing and Monitoring, Pergamon Press, London

Jackson School of Geoscience. "Some Useful Numbers on the Engineering Properties of Materials (Geologic and Otherwise)", from University of Texas https://www.jsg.utexas.edu/tyzhu/files/Some-Useful-Numbers.pdf

Japan Quality Assurance Organization (JQA) "Sonic Viewer-SX Ultrasonic Velocity Measuring System for Rock Sample", Japan: OYO Corporation, JQA-2772.

Jizba, D. (1991) "Mechanical and Acoustical Properties of Sandstones and Shales", (PhD thesis), Standford University.

Lake, L. (2007) "Petroleum Engineering Handbook", Society of Petroleum Engineers.

Mohamad, E. T., Kassim, K. A., and Komoo, I. (2005) "To Rip or To Blast: An Overview of Existing Excavation Assessment", Paper presented at the Brunei International Conference on Engineering and Technology, Brunei.

Onalo, D., Oloruntobi, O., Adidegba, S., Khan, F., James, L., and Butt, S. (2018) "Static Young's modulus model prediction for formation evaluation", Journal of Petroleum Science and Engineering, 171, pp394 - 402.

Romana, M. (1985) "New adjustment ratings for application of Bieniawski classification to slopes", Paper presented at the Proceedings of the International Symposium on the Role of Rock Mechanics in Excavations for Mining and Civil Works, Zacatecas, Mexico.

Sheorey, P. R. (1997) "Empirical Rock Failure Criteria". A.A. Balkema, Rotterdam.

Tate, R., Tan, D., and Ng, T. F. (Cartographer). (2008) "Geological Map of Peninsula Malaysia", Geological Society of Malaysia.

Yale, D. P., and Swami, V. (2017) "Conversion of dynamic mechanical property calculations to static values for geomechanical modeling", Am. Rock Mech. Assoc., Issues 17, pp644.